PHYSICAL REVIEW D **93,** 015018 (2016)

Looking for lepton flavor violation in supersymmetry at the LHC

Monoranjan Guchait,[1,*] Abhishek M. Iyer,[2,†] and Rickmoy Samanta[2,‡]
[1]*Department of High Energy Physics, Tata Institute of Fundamental Research, Homi Bhabha Road, Colaba, Mumbai 400 005, India*
[2]*Department of Theoretical Physics, Tata Institute of Fundamental Research, Homi Bhabha Road, Colaba, Mumbai 400 005, India*
(Received 3 December 2015; published 27 January 2016)

We consider models of supersymmetry that can incorporate sizeable mixing between different generations of sfermions. While the mixing is constrained by the nonobservation of various flavor-changing neutral current processes, there exist regions of the SUSY parameter space where the effects of such mixing can be probed at colliders. In this work, we explore this possibility by focusing on the slepton sector. The sleptons are produced through cascade decays in direct neutralino-chargino ($\chi_2^0\chi_1^\pm$) pair production at the Large Hadron Collider (LHC). The final state is characterized by three leptons and missing energy. We probe the lepton-flavor-violating (LFV) vertex arising in χ_2^0 decay by identifying a distinct and unambiguous combination of the trilepton final state containing a lepton pair with same flavor and same sign (SFSS) in addition to a pair with opposite flavor and opposite sign (OFOS). This combination of a trilepton final state containing both OFOS and SFSS pairs can not only suppress the SM background but also differentiate the flavor-violating decays of χ_2^0 from its corresponding flavor-conserving decays. We present results showing the sensitivity of lepton-flavor-violating parameters for a wide range of slepton and chargino-neutralino masses. In addition, we also illustrate signal significance for various points in the parameter space, taking into account background contributions assuming two luminosity options (100 and 1000 fb^{-1}) for the LHC run 2 experiment at $\sqrt{s} = 14$ TeV.

DOI: 10.1103/PhysRevD.93.015018

I. INTRODUCTION

The experiments dedicated to the investigation of flavor physics are considered to be one of the best indirect ways to establish the existence of new physics (NP). They play an important role in constraining the viability of various new physics scenarios, thereby complementing the direct collider searches. The effects which give rise to large flavor-changing neutral currents (FCNC) can also be potentially probed at the colliders. For instance, the possibility of observing a flavor-violating Higgs decay at the Large Hadron Collider (LHC) was discussed in [1–3]. Further, an observation of a 2.5σ excess in the $H \to \tau\mu$ channel by CMS [4] in the LHC experiment has generated a lot of interest in this topic and has led to a plethora of analyses [5–18]. The leptonic sector in the Standard Model (SM) is also interesting owing to the absence of FCNC. This can be attributed to the massless nature of neutrinos in the SM. The observation of neutrino oscillations led to a confirmation of the massive nature of left-handed neutrinos and consequently predicted a nonzero decay rate for rare processes like $\mu \to e\gamma$. The predicted branching ratio (BR) of this FCNC decay mode in the SM, however, is negligibly small ($\sim 10^{-40}$) due to the tiny neutrino mass and is beyond the sensitivity of the current flavor experiments. There exist several extensions of the SM which contribute to such rare processes via loops, thereby enhancing the BR substantially to $\sim 10^{-13}$–10^{-15}, which is expected to be within the reach of the indirect flavor probes. Needless to say, an observation of such processes is an unambiguous signal of the presence of physics beyond the SM. Therefore, looking for a signal of lepton flavor violation (LFV) directly or indirectly is a useful avenue to find NP. Following this argument, we explore the possibility of observing lepton flavor violation at the LHC.

There are several models in the literature which discuss the possibility of flavor violation in the leptonic sector. In the current analysis, we focus on the supersymmetric extension of the SM with soft masses having significant flavor mixing in the mass basis of fermions leading to new contributions to the BR of rare processes. For instance, soft masses with flavor mixing can arise in see-saw extensions of SUSY [19–21] and are also inspired by SUSY GUT [22–26]. Alternatively, introduction of flavor symmetries [27,28], models with messenger matter mixing in the gauge mediated supersymmetry breaking (GMSB) [29–33], models with R-symmetric supersymmetry [34,35], supersymmetric theories in the presence of extraspatial dimensions [36–44], *etc.* also lead to flavorful soft masses. Scenarios in which mass splitting leads to flavor violation have been considered in [31,45,46]. Such extensions, in general, lead to flavored soft masses and depending on the parameters

*guchait@tifr.res.in
†abhishek@theory.tifr.res.in
‡rickmoy@theory.tifr.res.in

can lead to observable rates for the flavor-violating decays in the squark and leptonic sector.

Flavor mixing in the sfermion mass matrices can be probed at the collider by the flavor-violating decay of a sparticle of flavor (say i) into a fermion of flavor j where $j \neq i$. Flavor-violating decays of sleptons were studied in the context of e^+e^- linear collider [47–53]. In Ref. [54] the authors studied the possibility of observing CP violation from slepton oscillations at the LHC and NLC. At the LHC, the sleptons can be produced either through Drell-Yan (DY) process or by the cascade decays from heavier sparticles. Flavor-violating decays of sleptons produced by DY were studied in [55,56], while those produced by cascade decays were studied in [57–63]. Probing LFV through the measurement of splitting in the mass eigenstates of sleptons was considered in [64–66]. In this paper we report on our study to detect flavor violation in the leptonic sector by producing sleptons in cascade decays through the pair production of a neutralino-chargino at the future LHC experiments with center of mass energy $\sqrt{s} = 14$ TeV.

Starting with the MSSM, we write the most general structure for the slepton mass matrix. The constraints on the model from the nonobservation of flavor-violating processes can be expressed by working in the mass-insertion approximation (MIA) [20,67] in terms of bounds on the flavor-violating parameter $\delta_{ij}, i \neq j$ as defined in Eq. (2) [68]. A nonzero δ_{ij} also opens up the possibility of flavor-violating decay as far as collider implications of flavored slepton masses are concerned.

Our goal is to probe the flavor-violating decay in the case of the first two generations in the slepton sector in SUSY. In this context, strong bounds exist on the flavor-violating parameter, coming primarily from the nonobservation of $\mu \to e\gamma$ decay [69]. There exist regions of parameter space where these bounds can be relaxed owing to the cancellations between different diagrams contributing to this process, thereby giving access to probe LFV at the colliders.

In this paper we explore this possibility of looking for LFV decays considering neutralino-chargino pair production in proton-proton collisions, which eventually lead to the final state consisting of three leptons and missing energy. The trilepton final state is characterized by the presence of two leptons with opposite flavor and opposite sign combination (OFOS). The presence of LFV in the trilepton final state is ensured by demanding a combination of a same-flavor–same-sign (SFSS) lepton pair along with the OFOS combination. While an imposition of this SFSS criteria along with OFOS has a tendency to decrease the signal, it aids in suppressing the backgrounds due to SM and SUSY significantly.

The paper is organized as follows: In Sec. II we discuss the model setup, introducing the various parameters relevant for the analysis in the framework of a simplified model. Relevant regions of parameter space consistent with the flavor constraints and conducive to be probed at the colliders are identified in this section. In Sec. III we explain our choice of the OFOS and SFSS combination to extract the signal with a detailed description of the simulation. The results of the simulation for the background and the representative points for the signal events are presented. In Sec. IV we show regions of the parameter space which can be probed at the LHC run 2 experiment in the near future. We conclude in Sec. V.

II. MODEL PARAMETRIZATION

In this section we introduce the basic model setup and related parameters necessary to describe LFV. In order to reduce the dependence on many parameters, we consider a simplified SUSY model (SMS) approach with only left-handed sleptons, a wino, and a bino while decoupling the rest of the spectrum. The μ term is assumed to be ~ 1 TeV to make the neutralino and chargino dominantly composed of gauginos with a very small higgsino component. In this case, the mass of the second lightest neutralino (χ_2^0,) and the lightest chargino ($\chi_1^\pm$,), are roughly the same as $\sim M_2$, the mass of the $SU(2)$ gauginos. The lightest neutralino (χ_1^0), which is assumed to be the lightest supersymmetric particle (LSP), has mass $\sim M_1$, the same as the mass of the $U(1)$ gaugino.

For the slepton sector, we focus on the flavor violation in the left-handed sector, making the right-handed sleptons very heavy, and set the left-right chiral mixing in the slepton mass matrix to be negligible. For simplicity, we assume only two generations. With these assumptions, the left-handed slepton mass matrix in the basis $l_F \equiv (\tilde{e}_F, \tilde{\mu}_F)$ is given as

$$\tilde{m}^2 = \begin{bmatrix} m^2_{L_{11}} & m^2_{L_{12}} \\ m^2_{L_{12}} & m^2_{L_{22}} \end{bmatrix}, \tag{1}$$

where F denotes the flavor basis (SUPER CKM) for the sleptons. In this basis, the flavor- violating parameter δ_{12} is parametrized as [20,67]

$$\delta_{12} = \frac{m^2_{L_{12}}}{\sqrt{m^2_{L_{11}} m^2_{L_{22}}}}. \tag{2}$$

Naturally, this flavor-violating parameter δ_{12} is coupled to the rates corresponding to flavor-violating rare decays in the first- and second-generation lepton sector. Hence, an upper bound on this parameter exists due to nonobservation of these rare decays like $\mu \to e\gamma$ [69], $\mu - e$ conversion [70], and $\mu \to eee$ [71].

In order to obtain the mass eigenvalues of the sleptons, the matrix in Eq. (1) can be rotated into a diagonal form by an angle θ given by

$$\sin 2\theta = \frac{2m^2_{L_{12}}}{m^2_{L_2} - m^2_{L_1}}, \tag{3}$$

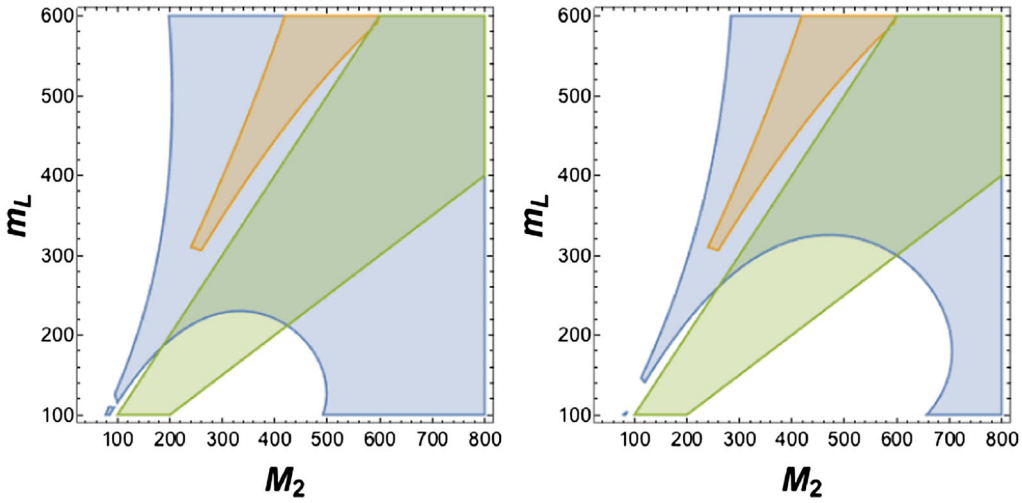

FIG. 1. Region satisfying Eqs. (11) and (12) (green), while the orange regions satisfy the $\mu \to e\gamma$ constraint for $\delta_{12} = 0.1$. The blue regions are allowed by the upper bound on BR $(\mu \to e\gamma)$ for $\delta_{12} = 0.01$ (left) and $\delta_{12} = 0.02$ (right). Units of mass are in GeV.

where $m^2_{L_i}$ are the eigenvalues. It can be related to the flavor-violating parameter δ_{12} as

$$\delta_{12} = \frac{\sin 2\theta (m^2_{L_2} - m^2_{L_1})}{2m^2_L}, \tag{4}$$

using $m_L = \frac{m_{L_1}+m_{L_2}}{2}$. The structure of the mass matrix, Eq. (1), allows for the possibility of flavor oscillations similar to neutrino flavor oscillations. The probability $P(\tilde{e}_F \to \mu)$ of a flavor eigenstate $\tilde{e}_F$ decaying into a muon is given by [49]

$$P(\tilde{e}_F \to \mu) = \sin^2 2\theta \frac{(\Delta m^2)^2}{4\Gamma^2 m^2_L + (\Delta m^2)^2} \mathrm{BR}(\tilde{\mu} \to \mu), \\ \sim \sin^2 2\theta \mathrm{BR}(\tilde{\mu} \to \mu) \quad \text{for } \Gamma m_L \ll \Delta m^2, \tag{5}$$

with $\Delta m^2 = m^2_{L_2} - m^2_{L_1}$. The above expression can be reexpressed in terms of the parameter δ_{12} from Eq. (4). Thus, the branching ratio for the flavor-violating decay $\chi^0_2 \to e\tilde{e} \to e\mu\chi^0_1$ can be computed as

$$\mathrm{BR}(\chi^0_2 \to e\mu\chi^0_1) = \mathcal{B}_{\mathrm{LFV}} \mathrm{BR}(\chi^0_2 \to \tilde{e}e) \mathrm{BR}(\tilde{e} \to e\chi^0_1) \\ + e \leftrightarrow \mu. \tag{6}$$

Here the suppression factor due to flavor violation is given by

$$\mathcal{B}_{\mathrm{LFV}} = \sin^2 2\theta = \left(\frac{m_L \delta_{12}}{\Delta m_{12}}\right)^2, \tag{7}$$

where $\Delta m_{12} = m_{L_2} - m_{L_1}$.

As mentioned before, bounds on δ_{12} and, hence, $\mathcal{B}_{\mathrm{LFV}}$ can be obtained by taking into account the experimental upper limit on the $\mathrm{BR}(\mu \to e\gamma) < 5.7 \times 10^{-13}$ [69]. The higher-dimensional operator contributing to this process is parametrized as [72]

$$\mathcal{L}_{FV} = e \frac{m_l}{2} \bar{e} \sigma_{\alpha\beta} (A_L P_L + A_R P_R) \mu F^{\alpha\beta}, \tag{8}$$

where the model dependence is captured by the Wilson coefficients $A_{L,R}$. The branching ratio for this process is then given by [72]

$$\mathrm{BR}(\mu \to e\gamma) = \frac{48\pi^3}{G_F^2} (|A_L|^2 + |A_R|^2). \tag{9}$$

In our considered model, $A_R \equiv 0$, as the right-handed sleptons are assumed to be very heavy. A_L, on the other hand, receives three contributions due to chargino, neutralino, and bino mediated diagrams and is given as [72]

$$A_L = \frac{\delta_{12}}{m^2_L} \left(\frac{\alpha_Y}{4\pi} f_n \left(\frac{M^2_1}{m^2_L} \right) + \frac{\alpha_Y}{4\pi} f_n \left(\frac{M^2_1}{m^2_L} \right) + \frac{\alpha_2}{4\pi} f_c \left(\frac{M^2_2}{m^2_L} \right) \right), \tag{10}$$

where $f_{n,c}$ are loop factors defined in [72] with a nontrivial mass dependence of related sparticles, and α_Y, α_2 are the $U(1)_Y$ and $SU(2)$ gauge couplings.

The analysis can be simplified again by choosing the following parametrization for the mass M_1 of the (LSP) χ^0_1,

$$M_1 = \frac{M_2}{2}, \tag{11}$$

which is the relation at the electroweak scale due to unification of gaugino masses at the GUT scale. For the sleptons we choose

$$M_2 > m_L > M_1. \tag{12}$$

This relation assumes that the intermediate sleptons in χ^0_2 decay are produced on-shell by requiring that they are lighter than the mass of $\chi^0_2 \simeq M_2$. Under these assumptions, we try to find the available range of parameters allowed by existing $\mu \to e\gamma$ constraints, as will be discussed later. Figure 1 shows the region in the $M_2 - m_L$ plane for which the conditions in Eqs. (11) and (12) are satisfied (green region). It depicts the region of parameter space which is of interest as far as collider implications are concerned, as discussed in this paper.

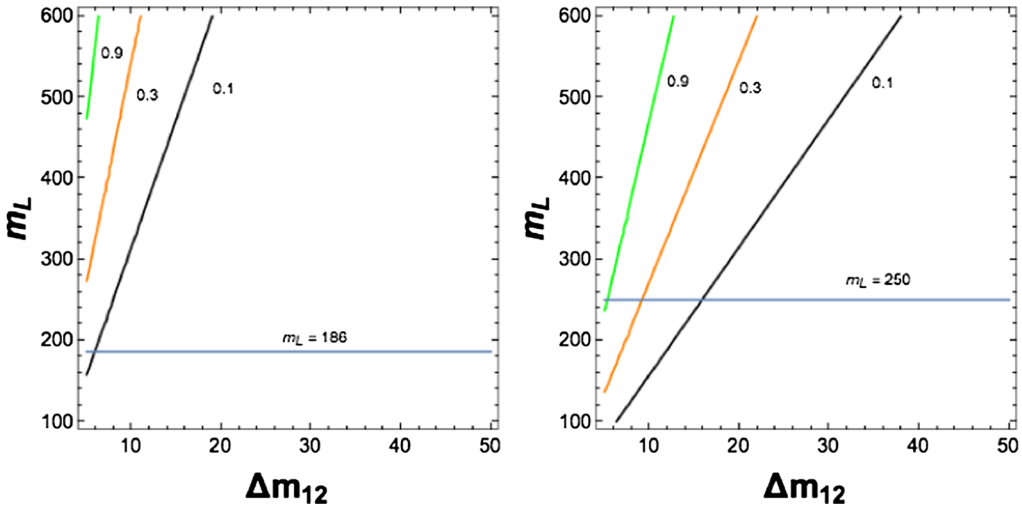

FIG. 2. Contours of $\mathcal{B}_{\rm LFV}$ for $\delta_{12} = 0.01$ (left) and $\delta_{12} = 0.02$ (right). The horizontal blue line is excluded by $\mathrm{BR}(\mu \to e\gamma)$ for $\delta_{12} = 0.01$ (left) and $\delta_{12} = 0.02$ (right). The units of mass are in GeV.

The blue region shows the parameter space for which $\mathrm{BR}(\mu \to e\gamma) < 5.7 \times 10^{-13}$ is satisfied for $\delta_{12} = 0.01(0.02)$ in the left (right) plot. As expected, due to the smaller value of δ_{12}, the blue region in the left plot has a larger overlap with the green region as compared to the plot in the right, thereby admitting smaller slepton masses. The orange region in both the plots shows the parameter space for which $\mathrm{BR}(\mu \to e\gamma) < 5.7 \times 10^{-13}$ is satisfied for $\delta_{12} = 0.1$. We find that there is virtually no overlap with the region which is of interest to us from the perspective of collider searches.

It would be interesting to estimate the suppression factor $\mathcal{B}_{\rm LFV}$ corresponding to the allowed region in the $M_2 - m_L$ plane for the values of δ_{12} in Fig. 1. As seen in Eq. (7), the parameter $\mathcal{B}_{\rm LFV}$, which affects the rate for LFV, is sensitive to the mass-splitting $\Delta m_{12} = m_{L_2} - m_{L_1}$ and m_L. $\mathcal{B}_{\rm LFV}$ increases with δ_{12} which can only be accommodated with a larger m_L. Thus, smaller values of δ_{12} are not conducive to generate a large $\mathcal{B}_{\rm LFV}$. $\mathcal{B}_{\rm LFV}$ is also inversely proportional to the mass splitting Δm_{12}. However, it cannot increase indefinitely as $\mathcal{B}_{\rm LFV} \leq 1$, leading to a lower bound on Δm_{12}. Figure 2 demonstrates the contours of constant $\mathcal{B}_{\rm LFV}$ in the $\Delta m_{12} - m_L$ plane. We find that for $\delta_{12} = 0.02$, sleptons in excess of 250 GeV are required to get $\mathcal{B}_{\rm LFV} \geq 0.1$, while being consistent with the flavor constraints (overlap of blue and green region) in Fig. 1.

III. SIGNAL AND BACKGROUND SIMULATIONS

As mentioned in the Introduction, we probe the signal of LFV in slepton decay, producing it via cascade decays of sparticles which are produced in proton-proton collisions at the LHC. Here we focus on $\chi_1^\pm \chi_2^0$ production which eventually leads to a trilepton final state as

$$pp \to \begin{cases} \chi_2^0 \to l_i^\pm \tilde{l}_i^\mp \to l_i^\pm l_j^\mp \chi_1^0, & i \neq j, \\ \chi_1^\pm \to l_i^\pm \nu \chi_1^0, \end{cases} \tag{13}$$

where i, j denote flavor indices (e, μ). The flavor-violating vertex causes the decay of a slepton $(\tilde{l}_i)$, coming from χ_2^0 decay, into a lepton of flavor l_j with $i \neq j$. It is clear from the above process that the signature of LFV is the presence of three leptons of which two leptons are with opposite flavor and opposite sign (OFOS) in addition to the missing energy ($\not{E}$) due to the presence of two LSPs and neutrinos. The leptons with OFOS originate from χ_2^0 decay while the third lepton comes from the $\chi_1^\pm$ decay. Thus, following this decay scenario, it is possible to have eight combinations of trileptons, each having at least one OFOS lepton pair as

$$\begin{aligned} &e^+e^+\mu^-; \quad e^-e^-\mu^+; \quad \mu^-e^+\mu^-; \quad \mu^+e^-\mu^+ \\ &e^+e^-\mu^+; \quad e^-e^+\mu^-; \quad \mu^+e^+\mu^-; \quad \mu^-e^-\mu^+. \end{aligned} \tag{14}$$

On the other hand, the pair production of $\chi_1^\pm \chi_2^0$ will also give rise to a trilepton final state with a flavor-conserving decay of χ_2^0 i.e. $\chi_2^0 \to l^+l^-\chi_1^0$. Note that this flavor-conserving decay scenario also results in eight combinations of trilepton final states given as

$$\begin{aligned} &e^+\mu^+\mu^-; \quad e^-\mu^+\mu^-; \quad \mu^-e^+e^-; \quad \mu^+e^+e^- \\ &\mu^+\mu^+\mu^-; \quad e^-e^+e^-; \quad e^+e^+e^-; \quad \mu^-\mu^-\mu^+, \end{aligned} \tag{15}$$

out of which four combinations of OFOS exist, as seen in the first line of Eq. (15). It is clearly a potential background corresponding to the signal channel in Eq. (14) and expected to have the same rate as the signal. However, a closer look at these two final states in Eqs. (14) and (15) reveals a characteristic feature. For example, in the case of the signal [Eq. (14)], out of the eight combinations of trileptons with OFOS combinations, notice that four combinations shown in the first line possess a pair of leptons with same flavor and same sign (SFSS) which are absent in the background final states shown in Eq. (15). The rest of the states with OFOS combination in Eq. (14) are identical to the final states given in Eq. (15). We exploit this

characteristic feature to extract the LFV signal events out of all three lepton events including all backgrounds. Thus our signal is composed of three leptons having combinations of both OFOS and SFSS together, which is an unambiguous and robust signature of LFV in SUSY. Note that while choosing a clean signature of LFV decay in SUSY, we pay a price by a factor of half as is clear from Eq. (14). However, this specific choice of combinations in trileptons is very powerful in eliminating much of the dominant SM backgrounds arising from WZ and $t\bar{t}$ following leptonic decays of W/Z and top quarks.

We now discuss our simulation strategy to estimate the signal rates while suppressing the SM and SUSY backgrounds. We performed simulations for both signal and background using PYTHIA8 [73] at 14 TeV center of mass energy and applying the following selections:

(i) *Jet selection*: The jets are reconstructed using FastJet [74] and based on anti k_T algorithm [75] setting the jet size parameter $R = 0.5$. The jets passing the cuts on transverse momentum $p_T^j \geq 30$ GeV, pseudorapidity $|\eta^j| \leq 3.0$, are accepted.

(ii) *Lepton selection*: Our signal event is composed of three leptons and are selected according to the following requirement on their transverse momenta and the pseudorapidity: $p_T^{\ell_{1,2,3}} \geq 20, 20, 10$ GeV; $|\eta^{\ell_{1,2,3}}| \leq 2.5$, where the leptons are p_T ordered with $p_T^{\ell_1}$ being the hardest one. In addition, the leptons are also required to be isolated i.e. free from nearby hadronic activities. It is ensured by requiring the total accompanying transverse energy, which is the scalar sum of transverse momenta of jets within a cone of size $\Delta R(l, j) \leq 0.3$ around the lepton, is less than 10% of the transverse momentum of the corresponding lepton.

(iii) *Missing transverse momentum*: We compute the missing transverse momentum by carrying out a vector sum over the momenta of all visible particles and then reverse its sign. Since $p_{\not{T}}$ is hard in signal events, so we apply a cut $p_{\not{T}} \geq 100$ GeV.

(iv) *Z mass veto*: We require that in three lepton events, the invariant mass of two leptons with opposite sign and same flavor should not lie in the mass window $m_{ll} = M_Z \pm 20$ GeV. It helps to get rid of significant amount of WZ background.

(v) *b like jet selection*: The b jets are identified through jet-quark matching; i.e., those jets which lie with in $\Delta R(b, j) < 0.3$ are assumed to be b like jets.

(vi) *OFOS*: Our signal event is characterized by the requirement that it has at least one lepton pair with opposite flavor and opposite sign.

(vii) *SFSS*: We require the presence of SFSS combination along with OFOS combination in three lepton final state, which is the characteristic of our signal. As stated before, this criteria is very effective in isolating the background due to the same SUSY process but for their subsequent flavor-conserving decays, in particular for χ_2^0 decay.

TABLE I. Representative choices of SUSY parameter space. All masses are in GeV.

Spectrum characteristics	A	B	C	D	E	F
$\chi_2^0/\chi_1^\pm$	210	314	417	518	619	718
χ_1^0	95.8	144	193	241	290	339
m_L	156	229	303	377	452	526
BR($\chi_2^0 \to \tilde{e}_L e$)	0.13	0.15	0.16	0.16	0.16	0.16
BR($\chi_2^0 \to \tilde{\mu}_L \mu$)	0.13	0.15	0.16	0.16	0.16	0.16

We perform our analysis by choosing various representative points in the SUSY parameter space. The spectrum is generated using SUSPECT [76] and the decays of the sparticles are computed using SUSYHIT [77]. Table I presents the six representative points (A–F) for which we discuss the details of our simulation. From A to F, the spectrum is characterized by increasing masses of gauginos, with the slepton mass m_L lying midway between the two, $m_L = (M_1 + M_2)/2$.

In Tables II and III we present the effects of the selection of cuts in simulation for both the signal and background, respectively. In addition to the SM backgrounds which are mainly due to $t\bar{t}$ and WZ, we also simulate the background taking into account the contributions due to flavor-conserving decay of χ_2^0 for each of the representative points in Table I. There are other subdominant backgrounds like tbW, ZZ where one lepton is missed or WW, if jets fake as leptons. However, these backgrounds are expected to be very small and not considered here. We present results for signals corresponding to those representative parameter space as shown in Table II. In this table, the first column shows the sequence of cuts applied in the simulation, while the remaining columns show event yields for the signal.

TABLE II. Event summary for signal after all selections. All energy units are in GeV.

	Signal($\chi_1^\pm \chi_2^0$)					
$M_2 \Rightarrow$	200	300	400	500	600	700
No. of events generated	10000	10000	10000	10000	10000	10000
$p_T^{\ell_{1,2}} > 20, p_T^{\ell_3} > 10$, $\lvert\eta\rvert < 2.5$	1371	1752	2014	2218	2225	2342
Lepton isolation cut	1330	1669	1883	2055	2036	2112
$p_{\not{T}} > 100$	474	959	1326	1600	1683	1860
OFOS	470	952	1319	1581	1659	1828
Z mass veto	423	849	1218	1485	1574	1752
SFSS	223	462	640	783	804	892
Case a: jet veto	91	205	288	337	346	380
Case b: b-like jet veto	221	458	635	777	798	884
Case c: $n_j \leq 1$ and b-like veto	161	375	479	604	617	687

TABLE III. Event summary for SUSY and SM background. All energy units are in GeV.

	SUSY($\chi_1^\pm\chi_2^0$)						SM	
	A	B	C	D	E	F	$t\bar{t}$	WZ
$M_2 \Rightarrow$	200	300	400	500	600	700	...	...
Cross section (fb) at 14 TeV	1.65×10^3	370.5	118.8	45.6	20.5	9.57	9.3×10^5	4.47×10^4
No. of events generated	10000	10000	10000	10000	10000	10000	10^7	3×10^6
$p_T^{\ell_{1,2}} > 20, p_T^{\ell_3} > 10, \lvert\eta\rvert < 2.5$	1299	1779	2015	2195	2245	2361	164895	23960
Lepton isolation cut	1251	1672	1874	2044	2051	2131	70233	22366
$\not{p}_T > 100$	454	967	1311	1624	1722	1872	19241	1669
OFOS	209	482	656	820	855	918	14012	858
Z mass veto	126	346	547	728	768	853	12395	122
SFSS	4	6	11	14	15	25	4598	22
Case a: jet veto	≤ 1	1	1	5	4	4	29	≤ 1
Case b: b-like jet veto	4	5	10	14	13	23	131	13
Case c: $n_j \leq 1$ and b-like veto	1	3	7	9	9	19	48	5

Table III presents the same for the backgrounds due to SUSY in the second column and the SM in the third column. Notice that lepton isolation requirement and a cut on $p_{\not{T}}$ has considerable impact in reducing $t\bar{t}$ and WZ background. As noted earlier, we find the SFSS criteria to be very effective in isolating the SUSY background due to flavor-conserving decay of χ_2^0 for all the representative points in Table I. Finally, it is possible to have large number of trilepton events in background processes, but imposition of specific choices like OFOS and SFSS, along with a large missing energy cut, help in isolating it to a great extent, as shown in Table III. In spite of this suppression of background events, the signal yields are far below the total background contribution, owing to the huge production cross sections, as shown in Table III. Therefore, in order to improve the signal sensitivity further, we impose additional requirements by looking into the other characteristics of signal events. For example, signal events are free from any kind of hadronic activities at the parton level; i.e., no hard jets are expected in the signal final state, whereas in background process, in particular, events from $t\bar{t}$ are accompanied by a large number of jets. We exploit this fact to increase signal sensitivity by adding the following criteria.

Case a: Jet veto

In this case we reject events if it contain any hard jets. In Table III we see that while the jet veto criteria reduces the $t\bar{t}$ and WZ background significantly, it also substantially damage the signal by a factor of 2 or 3 as shown in Table II. In signal process, jets arise mainly from the hadronic radiation in initial and final states and it is true for all the representative signal points. The reason can be attributed to enhancement of hadronic activities at higher energies. Nevertheless the jet veto seems to be useful to improve signal to background ratio. However we consider two more alternatives with a goal to increase signal sensitivity further:

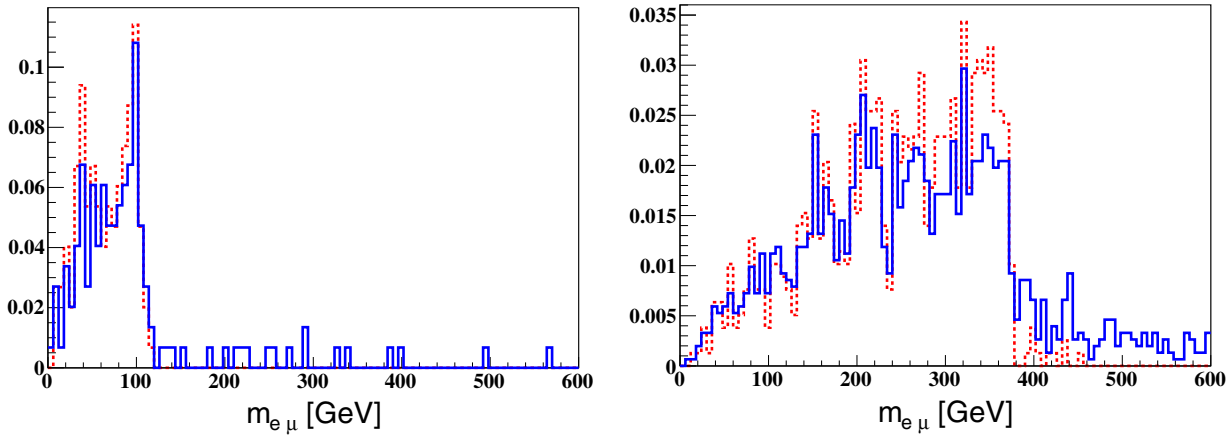

FIG. 3. The OFOS dilepton invariant mass distribution for spectrum A (left) and spectrum F (right). The events are selected at the SFSS level.

TABLE IV. Normalized cross section (fb) and $S/\sqrt{B}$ for signal and background subject to three selection conditions.

	Signal (S)						Background (B)	
Properties	A	B	C	D	E	F	$t\bar{t}$	WZ
Cross section (fb) at 14 TeV	1.65×10^3	370.5	118.8	45.6	20.5	9.57	9.3×10^5	4.47×10^4
				Normalized cross sections				
Case a: jet veto	15.01	7.59	3.41	1.51	0.67	0.37	2.69	≤ 1
Case b: b-like veto	36.4	16.9	7.54	3.54	1.63	0.85	12.1	0.19
Case c: $n_j \leq 1$ and b-like veto	26.5	13.9	5.7	2.75	1.26	0.66	4.4	0.07
				$\frac{S}{\sqrt{B}}$(@100) fb^{-1}				
Case a: jet veto	91.43	45.93	20.78	9.32	4.31	2.24	⋯	⋯
Case b: b-like veto	100.99	47.87	21.34	10.04	4.64	2.43	⋯	⋯
Case c: $n_j \leq 1$ and b-like veto	122.4	64.4	26.4	12.8	5.92	3.12	⋯	⋯

Case b: b-like jet veto

Here we eliminate events if there be at least one b like jet. As can be seen Table III, b jet veto is more efficient than the jet veto condition, as the $t\bar{t}$ background is suppressed by a few orders of magnitude without costing the signal too much.

Case c: Apply b-like jet veto and number of jets $n_j \leq 1$

Here we apply the b-like jet veto condition along with the presence of maximum one jet. As seen in Table III, it is very helpful in reducing the $t\bar{t}$ background significantly, but it does not affect the signal as much as the simple jet veto condition ($n_j = 0$) does alone.

Note that we have identified b-like jets by a naive jet-quark matching which is an overestimation from the realistic b-jet tagging [78] which is out of scope of the present analysis. However, for the sake of illustration, we present these results with b-jet veto [cases (b) and (c)] to demonstrate that this criteria might be very useful in suppressing backgrounds, which requires more detector based simulation. In view of this, we focus only on the results obtained by using jet veto, case (a), for further discussion.

We also present the dilepton ($e\mu$) invariant mass distributions for the spectrum A (left) and F (right) in Fig. 3 normalizing it to unity. It is subject to all primary selection cuts on leptons and jets, including the OFOS and SFSS combination. The $m_{e\mu}$ distribution is expected to have a sharp edge on higher side, which can be derived analytically from kinematical consideration. The position of this edge of $m_{e\mu}$ is given as [59,79],

$$(m_{e\mu}^{\max})^2 = m_{\chi_2^0}^2 \left(1 - \frac{m_L^2}{m_{\chi_2^0}^2}\right)\left(1 - \frac{m_{\chi_1^0}^2}{m_L^2}\right). \qquad (16)$$

The appearance of an edge in the $m_{e\mu}$ distribution is a clear indication of LFV vertex in the χ_2^0 decay. However, this $m_{e\mu}$ distribution is affected by a combinatorial problem. For each trilepton event, two OFOS pairs can be constructed: (a) both leptons coming from χ_2^0 decay and (b) an "imposter" pair with one lepton from χ_2^0 and the other from $\chi_1^\pm$. In Fig. 3 the red (dotted) curve represents the dilepton invariant mass distribution of the leptons tracked to the χ_2^0 vertex while blue (solid) curve corresponds to dilepton without any prior information about their origin. It (red dotted line) exhibits a very distinct edge as the identity of the lepton pair originating for χ_2^0 is known *a priori*. The (solid) blue line is more realistic as it includes both the correct OFOS and SFSS pair as well as the contamination due to the "impostor" pair which is responsible for a tail beyond the edge. As a result it exhibits a more diffused behavior near the position of the edge. However, we can roughly estimate the position of the edge using the blue (solid) line as ∼120 GeV for the left panel and ∼375 GeV for the right panel. We find that these values are in fairly good agreement with the corresponding numbers used in our simulation. It may be noted here that such distributions with a sharp edge are the characteristic feature of these type of decays which can also be exploited to suppress backgrounds [59] in order to increase signal to background ratio.

IV. RESULTS AND DISCUSSIONS

Table IV gives the normalized signal and background cross sections due to all selection cuts. These are obtained by multiplying the production cross section given in the first row by acceptance efficiencies. The production cross section are estimated by multiplying the leading-order (LO) cross section obtained from PYTHIA8 with the corresponding k factors.[1] Corresponding to these signal and background cross sections, we also present the signal significance by computing $S/\sqrt{\mathrm{B}}$ for integrated luminosity 100 fb^{-1} as shown in the bottom of Table IV. Although case (b) corresponding to b-like jet veto results in the largest cross section for all signal parameter space, signal significance does not improve due to comparatively less suppression of SM backgrounds. With the increase of gaugino masses acceptance efficiencies goes up as final state

[1]The appropriate k factors for $t\bar{t}$ and WZ processes are 1.6 [80] and 1.7 [81], respectively, while for the signal it is 1.5 [82].

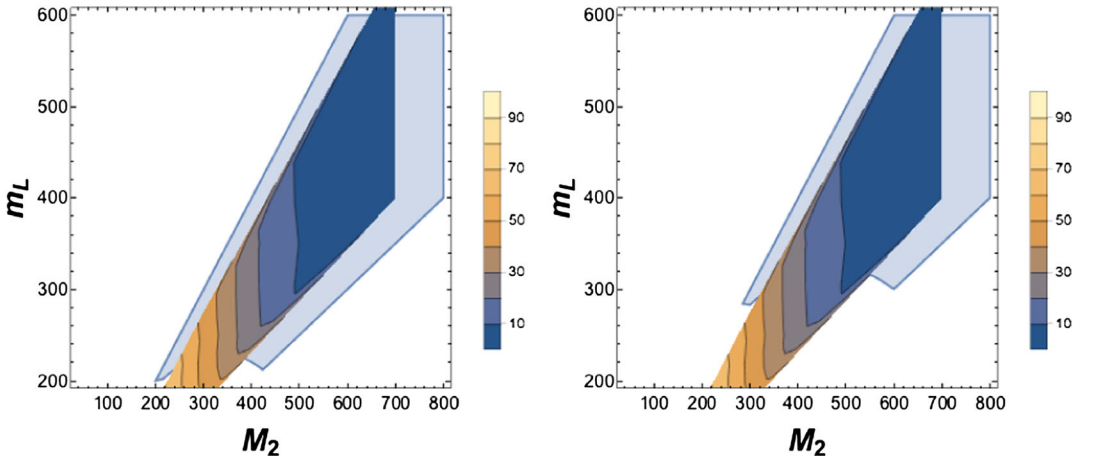

FIG. 4. Variation of $S/\sqrt{B}$ (using jet veto, case (a), for different regions with two choices of $\delta_{12} = 0.01$ (left) and $\delta_{12} = 0.02$ (right). The light blue regions are allowed by the BR $(\mu \to e\gamma)$ constraint. Here we assume $\mathcal{B}_{\rm LFV} = 1$. Masses are in GeV.

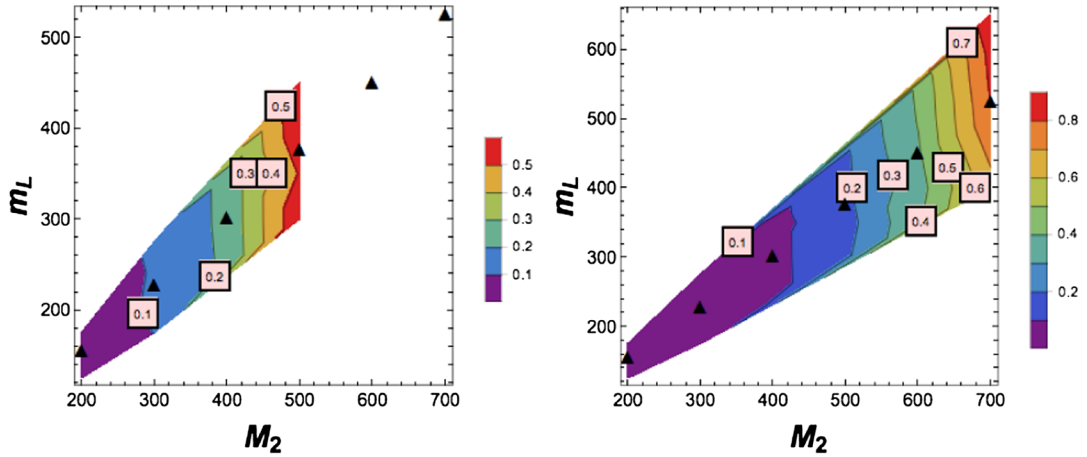

FIG. 5. Minimum value (in small box) of $\mathcal{B}_{\rm LFV}$ for a $S/\sqrt{B} = 5$ discovery for $\mathcal{L} = 100$ fb^{-1} (left) and $\mathcal{L} = 1000$ fb^{-1} (right). The $S/\sqrt{B}$ is computed using jet veto condition. The filled triangles correspond to the representative points A-F from left to right. The plot is truncated at the point where $\mathcal{B}_{\rm LFV} > 1$ is required to get a 5σ sensitivity of signal for that particular luminosity. Masses are in GeV.

particles become comparatively harder, but $S/\sqrt{B}$ is depleted due to drop in $\chi_1^\pm\chi_2^0$ pair production cross section. While estimating signal rates and significance, we assume a maximal flavor violation i.e. $\mathcal{B}_{\rm LFV} = 1$. Obviously, a further suppression is expected by a factor $\mathcal{B}_{\rm LFV}$ which depletes the BR of χ_2^0, [see Eq. (6)]. For a given δ_{12}, $\mathcal{B}_{\rm LFV}$ is a function of the slepton mass as well as the mass splitting Δm_{12} as shown in Fig. 2. For instance $S/\sqrt{B}$ may suffer by an order of magnitude for $\mathcal{B}_{\rm LFV} = 0.1$. While the lower end of the spectrum can lead to a larger $S/\sqrt{B}$, the corresponding $\mathcal{B}_{\rm LFV}$ decreases as we move further towards the IR part of the slepton spectrum. This can be attributed to stronger bounds on δ_{12} for lower slepton masses. Though the lower mass is not yet ruled out, it is more economical to consider relatively heavier slepton masses as the bounds from current and future experiments will be relatively weaker.

In Fig. 4, we illustrate this mass sensitivity by presenting $S/\sqrt{B}$ obtained using jet veto condition case as presented by case (a). Notice that for a given $\chi_1^\pm$ and χ_2^0 masses, signal is not very sensitive to slepton mass as long as it is produced on-shell from χ_2^0 decay and $M_2 - m_L$ is sufficiently high. The regions in the $M_2 - m_L$ plane correspond to different values of $S/\sqrt{B}$ computed for $\mathcal{L} = 100$ fb^{-1} and by assuming $\mathcal{B}_{\rm LFV} = 1$. The sleptons and gaugino masses follow the parametrization in Eqs. (11) and (12). Note that the parametrization used in Table I for the slepton masses has been relaxed in Fig. 4. It is superimposed on the region satisfying $\mathrm{BR}(\mu \to e\gamma) < 5.7 \times 10^{-13}$ for $\delta_{12} = 0.01$ (left) and $\delta_{12} = 0.02$ (right).[2] As seen from Table IV and Fig. 4, the signal significance is better for lower masses due to the larger $\chi_1^\pm\chi_2^0$ pair production cross section. However, it suffers from smaller values of $\mathcal{B}_{\rm LFV}$ corresponding to those slepton masses as shown in Eq. (7) and Fig. 2.

Figure 5 shows the sensitivity reach of $\mathcal{B}_{\rm LFV}$ in the $M_2 - m_L$ plane using the parametrization in Eqs. (11) and (12). The numbers in boxes for different colored regions present

[2]We note here that for the approximation of Eq. (5) to be valid for $\mathcal{B}_{\rm LFV} = 1$, $\delta_{12} \gg 0.005$ for the lowest masses [49]. As the mass increases, this lower bound is considerably relaxed.

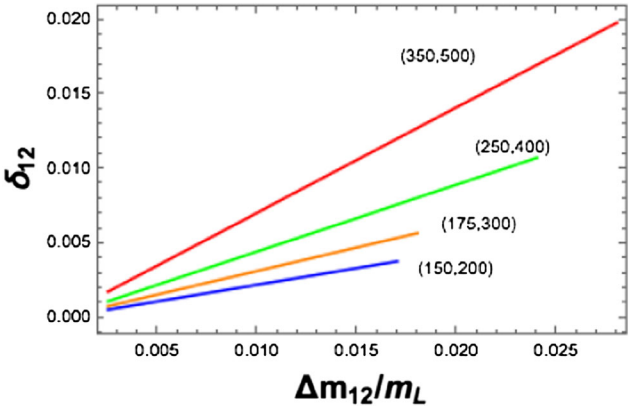

FIG. 6. Variation of δ_{12} as a function of $\frac{\Delta m}{m_L}$ for different choices of (m_L, M_2) and $\mathcal{L} = 100$ fb^{-1}. Each line is discontinued at the point where the δ_{12} exceeds the current experimental bound $\mu \to e\gamma$ for the given mass.

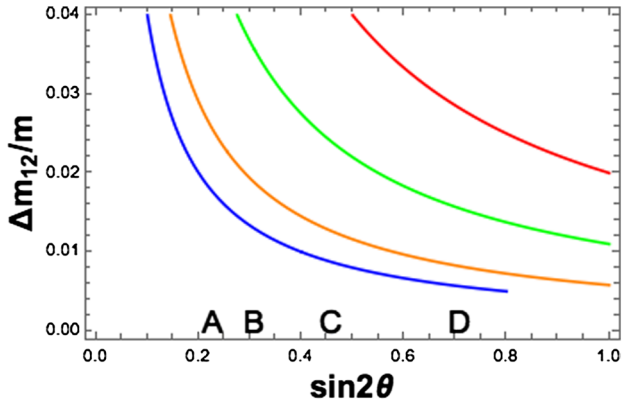

FIG. 7. The lines represent the constant contours of BR $(\mu \to e\gamma) = 5.7 \times 10^{-13}$ for the four mass points in Fig. 6. The region above the contour is excluded. The color coding for the contours representing different (m_L, M_2) values is same as in Fig. 6. The position of the points A–D corresponds to the minimum $\sin 2\theta$ required for a 5σ discovery for $\mathcal{L} = 100$ fb^{-1} with the outermost point corresponding to the heavier spectrum.

the minimum values of $\mathcal{B}_{\rm LFV}$ which can be probed, requiring a 5σ discovery of the trilepton signal at the LHC and are presented for two different luminosity options: $\mathcal{L} = 100$ fb^{-1} (left) and $\mathcal{L} = 1000$ fb^{-1} (right). As seen in Figs. 1 and 2, with the constraints from indirect flavor measurements getting tighter, larger $\mathcal{B}_{\rm LFV}$ can be attained with heavier slepton masses, while respecting bounds from the rare decays. For example, for lower masses $\chi_2^0 \sim \chi_1^\pm \sim 250$ GeV and $m_L \sim 200$ GeV, the LFV parameter $\mathcal{B}_{\rm LFV} \sim 0.05$ or more can be probed at 5σ level of signal sensitivity for $\mathcal{L} = 100$ fb^{-1}. As expected, the sensitivity of $\mathcal{B}_{\rm LFV}$ measurement goes up with the increase of gaugino and slepton masses which can be attributed to the drop in cross sections. The left plot in Fig. 5 is terminated at the point corresponding to a requirement of $\mathcal{B}_{\rm LFV} = 1$ for a 5σ discovery. As a result, the representative points E and F corresponding to heavier slepton masses are beyond the sensitivity of LHC at $\mathcal{L} = 100$ fb^{-1} as they require $\mathcal{B}_{\rm LFV} > 1$ to achieve a 5σ discovery. However, flavor-violating decays with heavier slepton masses as high as 650 GeV can be probed with an integrated luminosity of $\mathcal{L} = 1000$ fb^{-1} as shown in the right plot of Fig. 5. The interplay between the sensitivity of $\mathcal{B}_{\rm LFV}$ at the LHC for a given slepton mass and it's consistency with the upper bound on the $\mu \to e\gamma$, is given in Fig. 6. Note that the sensitivity of the $\mathcal{B}_{\rm LFV}$ and the upper limit on the flavor-violating parameter δ_{12} are a function of the slepton mass. In Fig. 6, we present the contours in the $\delta_{12} - \frac{\Delta m}{m_L}$ plane for various combination of values of (m_L, M_2). The contours are governed by Eq. (7) with the slope given by $\sin 2\theta = \sqrt{\mathcal{B}_{\rm LFV}}$, the value of which is determined from Fig. 5 requiring a 5σ sensitivity at $\mathcal{L} = 100$ fb^{-1}. This plot is obtained by varying Δm_{12} and terminating it at the point for which the corresponding δ_{12} for a given set of (m_L, M_2) violates the upper bound on $\mu \to e\gamma$. Since large mixing angle leads a larger contribution to $\mu \to e\gamma$, it must be compensated by a correspondingly smaller mass splitting. This corresponds to a smaller off-diagonal element $m^2_{L_{12}}$ in Eq. (1). This is clearly evident in Fig. 6 where larger splitting are permitted for larger slepton masses as compared to lighter ones. Note that the region below the lines is beyond the sensitivity of the LHC at $\mathcal{L} = 100$ fb^{-1}.

Figure 7 depicts contours of BR $(\mu \to e\gamma) = 5.7 \times 10^{-13}$ in the $\sin 2\theta - \Delta m/m$ plane corresponding to the four mass points in Fig. 6, with the outermost contour corresponding to $(m_L, M_2) = (350, 500)$. The region above the contours are excluded as they exceed the upper bound on the $\mu \to e\gamma$ branching fraction. The black points in the figure represent the minimum $\sin 2\theta$ that can be probed at 5σ level for $\mathcal{L} = 100$ fb^{-1} integrated luminosity, with the outermost point corresponding to the heaviest spectrum point in Fig. 6. We see that they are well within the contours satisfying the $\mu \to e\gamma$ bound.

V. CONCLUSION

The observation of flavor-violating rare decays would be one of the best indicators of the existence of physics beyond the SM. Measurements of such decays play an important role in constraining several new physics models and hence has received a lot of attention recently. We attempt to explore the flavor violation in the lepton sector in the context of well motivated models of flavorful supersymmetry. We follow an approach based on a simplified model with only the left-handed sleptons along with the neutralinos which are gaugino dominated. We consider pair production of $\chi_2^0\chi_1^\pm$ and their subsequent leptonic decays including the LFV decays of χ_2^0. The final state is composed of three leptons and accompanied by a large missing energy. In addition to the presence of a lepton pair with

OFOS, we observed that certain trilepton combinations are also characterized by a lepton pair with SFSS, which is a unique and robust signature of LFV in SUSY.

The discovery potential of observing this LFV signal is dependent on the masses of sleptons and gauginos and the flavor-violating parameter $\mathcal{B}_{\rm LFV}$. However, these masses are constrained by nonobservation of FCNC decays such as $\mu \to e\gamma$ and they get more severely constrained as the flavor-violating parameter δ_{12} becomes larger. We have identified the allowed ranges of slepton and gaugino masses relevant for our study. The key feature of this analysis is to probe LFV signal at the LHC and find the sensitivity of the lepton-flavor-violating parameter $\mathcal{B}_{\rm LFV}$ while respecting the constraints from the processes like $\mu \to e\gamma$. We explore this LFV signal through trilepton final state via chargino-neutralino pair production, thereby predicting the reach of $\mathcal{B}_{\rm LFV}$. In addition variation of LFV parameter $\mathcal{B}_{\rm LFV}$ with masses of slepton and mass difference between slepton mass eigenstates (Δm_{12}) are also presented.

Estimating the contributions due to various background processes, we predict the signal sensitivity for a few representative choices of SUSY parameters. The combination of three leptons with OFOS and SFSS is found to be very useful to achieve a reasonable sensitivity. It is found that for gaugino masses ~250 GeV and slepton masses ~200 GeV, the LFV parameter $\mathcal{B}_{\rm LFV}$ as low as 0.05 can be probed with 100 fb^{-1} integrated luminosity. For heavier masses ~600–700 GeV, because of reduced $\chi_1^{\pm}\chi_2^0$ pair production cross section, the measurement of LFV parameter $\mathcal{B}_{\rm LFV}$ requires higher luminosity ~1000 fb^{-1}. Our study clearly establishes the prospects of finding LFV signal in this SUSY channel at the LHC run 2 experiment with high luminosity options.

ACKNOWLEDGMENTS

A. I. and R. S. would like to thank Debjyoti Bardhan and Sanmay Ganguly for discussions.

[1] J. L. Diaz-Cruz and J. Toscano, Lepton flavor violating decays of Higgs bosons beyond the standard model, Phys. Rev. D **62**, 116005 (2000).
[2] G. Blankenburg, J. Ellis, and G. Isidori, Flavour-changing decays of a 125 GeV Higgs-like particle, Phys. Lett. B **712**, 386 (2012).
[3] R. Harnik, J. Kopp, and J. Zupan, Flavor violating Higgs decays, J. High Energy Phys. 03 (2013) 026.
[4] V. Khachatryan *et al.* (CMS Collaboration), Search for lepton flavour violating decays of the Higgs boson, Phys. Lett. **B749**, 337 (2015).
[5] A. Pilaftsis, Lepton flavor nonconservation in H0 decays, Phys. Lett. B **285**, 68 (1992).
[6] A. Brignole and A. Rossi, Lepton flavor violating decays of supersymmetric Higgs bosons, Phys. Lett. B **566**, 217 (2003).
[7] E. Arganda, A. M. Curiel, M. J. Herrero, and D. Temes, Lepton flavor violating Higgs boson decays from massive seesaw neutrinos, Phys. Rev. D **71**, 035011 (2005).
[8] A. Azatov, M. Toharia, and L. Zhu, Higgs mediated FCNC's in warped extra dimensions, Phys. Rev. D **80**, 035016 (2009).
[9] A. Arhrib, Y. Cheng, and O. C. Kong, Higgs to $\mu + \tau$ decay in supersymmetry without R-parity, Europhys. Lett. **101**, 31003 (2013).
[10] A. Falkowski, D. M. Straub, and A. Vicente, Vector-like leptons: Higgs decays and collider phenomenology, J. High Energy Phys. 05 (2014) 092.
[11] M. Arana-Catania, E. Arganda, and M. Herrero, Non-decoupling SUSY in LFV Higgs decays: A window to new physics at the LHC, J. High Energy Phys. 09 (2013) 160.
[12] M. Arroyo, J. L. Diaz-Cruz, E. Diaz, and J. A. Orduz-Ducuara, Flavor violating Higgs signals in the texturized two-Higgs doublet model (2HDM-Tx), arXiv:1306.2343.
[13] E. Arganda, M. Herrero, X. Marcano, and C. Weiland, Imprints of massive inverse seesaw model neutrinos in lepton flavor violating Higgs boson decays, Phys. Rev. D **91**, 015001 (2015).
[14] D. Aristizabal Sierra and A. Vicente, Explaining the CMS Higgs flavor violating decay excess, Phys. Rev. D **90**, 115004 (2014).
[15] J. Heeck, M. Holthausen, W. Rodejohann, and Y. Shimizu, Higgs $\to \mu\tau$ in Abelian and non-Abelian flavor symmetry models, Nucl. Phys. **B896**, 281 (2015).
[16] C.-J. Lee and J. Tandean, Lepton-flavored scalar dark matter with minimal flavor violation, J. High Energy Phys. 04 (2015) 174.
[17] A. Crivellin, G. D'Ambrosio, and J. Heeck, Explaining $h \to \mu^{\pm}\tau^{\mp}$, $B \to K^*\mu^+\mu^-$ and $B \to K\mu^+\mu^-/B \to Ke^+e^-$ in a Two-Higgs-Doublet Model with Gauged $L_\mu - L_\tau$, Phys. Rev. Lett. **114**, 151801 (2015).
[18] L. de Lima, C. S. Machado, R. D. Matheus, and L. A. F. do Prado, Higgs flavor violation as a signal to discriminate models, J. High Energy Phys. 11 (2015) 074.
[19] F. Borzumati and A. Masiero, Large Muon and Electron Number Violations in Supergravity Theories, Phys. Rev. Lett. **57**, 961 (1986).
[20] L. J. Hall, V. A. Kostelecky, and S. Raby, New flavor violations in supergravity models, Nucl. Phys. **B267**, 415 (1986).
[21] A. Masiero, S. K. Vempati, and O. Vives, Massive neutrinos and flavor violation, New J. Phys. **6**, 202 (2004).

[22] A. Masiero, S. K. Vempati, and O. Vives, Seesaw and lepton flavor violation in SUSY SO(10), Nucl. Phys. **B649**, 189 (2003).
[23] A. Masiero, S. K. Vempati, and O. Vives, Flavour physics and grand unification, *Particle physics beyond the standard model. Proceedings, Summer School on Theoretical Physics, 84th Session, Les Houches, France* (2005), p. 1.
[24] L. Calibbi, A. Faccia, A. Masiero, and S. Vempati, Lepton flavour violation from SUSY-GUTs: Where do we stand for MEG, PRISM/PRIME and a super flavour factory, Phys. Rev. D **74**, 116002 (2006).
[25] M. Hirsch, F. Joaquim, and A. Vicente, Constrained SUSY seesaws with a 125 GeV Higgs, J. High Energy Phys. 11 (2012) 105.
[26] L. Calibbi, D. Chowdhury, A. Masiero, K. Patel, and S. Vempati, Status of supersymmetric type-I seesaw in SO(10) inspired models, J. High Energy Phys. 11 (2012) 040.
[27] J. L. Feng, C. G. Lester, Y. Nir, and Y. Shadmi, The Standard Model and supersymmetric flavor puzzles at the Large Hadron Collider, Phys. Rev. D **77**, 076002 (2008).
[28] J. L. Feng, S. T. French, I. Galon, C. G. Lester, Y. Nir, Y. Shadmi, D. Sanford, and F. Yu, Measuring slepton masses and mixings at the LHC, J. High Energy Phys. 01 (2010) 047.
[29] B. Fuks, B. Herrmann, and M. Klasen, Flavour violation in gauge-mediated supersymmetry breaking models: Experimental constraints and phenomenology at the LHC, Nucl. Phys. **B810**, 266 (2009).
[30] Y. Shadmi and P. Z. Szabo, Flavored gauge-mediation, J. High Energy Phys. 06 (2012) 124.
[31] M. Abdullah, I. Galon, Y. Shadmi, and Y. Shirman, Flavored gauge mediation, a heavy Higgs, and supersymmetric alignment, J. High Energy Phys. 06 (2013) 057.
[32] L. Calibbi, P. Paradisi, and R. Ziegler, Gauge mediation beyond minimal flavor violation, J. High Energy Phys. 06 (2013) 052.
[33] L. Calibbi, P. Paradisi, and R. Ziegler, Lepton flavor violation in flavored gauge mediation, Eur. Phys. J. C **74**, 3211 (2014).
[34] G. D. Kribs, E. Poppitz, and N. Weiner, Flavor in supersymmetry with an extended R-symmetry, Phys. Rev. D **78**, 055010 (2008).
[35] G. D. Kribs, A. Martin, and T. S. Roy, Squark flavor violation at the LHC, J. High Energy Phys. 06 (2009) 042.
[36] Y. Nomura, M. Papucci, and D. Stolarski, Flavorful supersymmetry, Phys. Rev. D **77**, 075006 (2008).
[37] Y. Nomura and D. Stolarski, Naturally flavorful supersymmetry at the LHC, Phys. Rev. D **78**, 095011 (2008).
[38] Y. Nomura, M. Papucci, and D. Stolarski, Flavorful supersymmetry from higher dimensions, J. High Energy Phys. 07 (2008) 055.
[39] D. Marti and A. Pomarol, Supersymmetric theories with compact extra dimensions in $N = 1$ superfields, Phys. Rev. D **64**, 105025 (2001).
[40] K.-w. Choi, D. Y. Kim, I.-W. Kim, and T. Kobayashi, Supersymmetry breaking in warped geometry, Eur. Phys. J. C **35**, 267 (2004).
[41] J.-d. Choi and S.-T. Hong, Warped product approach to universe with nonsmooth scale factor, J. Math. Phys. (N.Y.) **45**, 642 (2004).
[42] E. Dudas, G. von Gersdorff, J. Parmentier, and S. Pokorski, Flavour in supersymmetry: Horizontal symmetries or wave function renormalisation, J. High Energy Phys. 12 (2010) 015.
[43] A. M. Iyer and S. K. Vempati, Warped alternatives to Froggatt-Nielsen models, Phys. Rev. D **88**, 016005 (2013).
[44] A. M. Iyer, V. S. Mummidi, and S. K. Vempati, Gravitational rescue of minimal gauge mediation, arXiv:1408.4462.
[45] I. Galon, G. Perez, and Y. Shadmi, Non-degenerate squarks from flavored gauge mediation, J. High Energy Phys. 09 (2013) 117.
[46] L. Calibbi, A. Mariotti, C. Petersson, and D. Redigolo, Selectron NLSP in gauge mediation, J. High Energy Phys. 09 (2014) 133.
[47] N. Krasnikov, Flavor lepton number violation at LEP-2, Mod. Phys. Lett. A **09**, 791 (1994).
[48] N. Krasnikov, Search for flavor lepton number violation in slepton decays at LEP-2 and NLC, Phys. Lett. B **388**, 783 (1996).
[49] N. Arkani-Hamed, H.-C. Cheng, J. L. Feng, and L. J. Hall, Probing Lepton Flavor Violation at Future Colliders, Phys. Rev. Lett. **77**, 1937 (1996).
[50] J. Hisano, M. M. Nojiri, Y. Shimizu, and M. Tanaka, Lepton flavor violation in the left-handed slepton production at future lepton colliders, Phys. Rev. D **60**, 055008 (1999).
[51] M. Guchait, J. Kalinowski, and P. Roy, Supersymmetric lepton flavor violation in a linear collider: The Role of charginos, Eur. Phys. J. C **21**, 163 (2001).
[52] E. Carquin, J. Ellis, M. Gomez, and S. Lolab, Searches for lepton flavour violation at a linear collider, J. High Energy Phys. 11 (2011) 050.
[53] A. Abada, A. Figueiredo, J. Romao, and A. Teixeira, Lepton flavour violation: Physics potential of a Linear Collider, J. High Energy Phys. 08 (2012) 138.
[54] N. Arkani-Hamed, J. L. Feng, L. J. Hall, and H.-C. Cheng, *CP* violation from slepton oscillations at the LHC and NLC, Nucl. Phys. **B505**, 3 (1997).
[55] S. Bityukov and N. Krasnikov, The Search for sleptons and flavor lepton number violation at LHC (CMS), Phys. At. Nucl. **62**, 1213 (1999).
[56] N. Krasnikov, Search for flavor lepton number violation in slepton decays at LHC, JETP Lett. **65**, 148 (1997).
[57] K. Agashe and M. Graesser, Signals of supersymmetric lepton flavor violation at the CERN LHC, Phys. Rev. D **61**, 075008 (2000).
[58] I. Hinchliffe and F. Paige, Lepton flavor violation at the CERN LHC, Phys. Rev. D **63**, 115006 (2001).
[59] J. Hisano, R. Kitano, and M. M. Nojiri, Slepton oscillation at large hadron collider, Phys. Rev. D **65**, 116002 (2002).
[60] R. Kitano, A clean slepton mixing signal at the LHC, J. High Energy Phys. 03 (2008) 023.
[61] S. Kaneko, J. Sato, T. Shimomura, O. Vives, and M. Yamanaka, Measuring lepton flavour violation at LHC with long-lived slepton in the coannihilation region, Phys. Rev. D **87**, 039904 (2013).
[62] Y. Andreev, S. Bityukov, N. Krasnikov, and A. Toropin, Using the $e^{+/-}\mu^{+/-} + E_T^{\mathrm{miss}}$ signature in the search for

supersymmetry and lepton flavour violation in neutralino decays, Phys. At. Nucl. **70**, 1717 (2007).
[63] F. Deppisch, Lepton flavor violation at the LHC, SUSY 2007 proceedings, 15th International Conference on Supersymmetry and Unification of Fundamental Interactions, Karlsruhe, Germany (2007).
[64] B. Allanach, J. Conlon, and C. Lester, Measuring smuon-selectron mass splitting at the CERN LHC and patterns of supersymmetry breaking, Phys. Rev. D **77**, 076006 (2008).
[65] A. J. Buras, L. Calibbi, and P. Paradisi, Slepton mass-splittings as a signal of LFV at the LHC, J. High Energy Phys. 06 (2010) 042.
[66] I. Galon and Y. Shadmi, Kinematic edges with flavor splitting and mixing, Phys. Rev. D **85**, 015010 (2012).
[67] F. Gabbiani and A. Masiero, FCNC in generalized supersymmetric theories, Nucl. Phys. **B322**, 235 (1989).
[68] F. Gabbiani, E. Gabrielli, A. Masiero, and L. Silvestrini, A complete analysis of FCNC and *CP* constraints in general SUSY extensions of the standard model, Nucl. Phys. **B477**, 321 (1996).
[69] J. Adam *et al.*, New Constraint on the Existence of the $\mu^+ \to e^+\gamma$ Decay, Phys. Rev. Lett. **110**, 201801 (2013).
[70] P. Wintz *et al.* (SINDRUM II Collaboration), Test of LFC in $\mu - e$ conversion on titanium (1996), p. 458.
[71] M. De Gerone, $\mu \to e\gamma$ and $\mu \to eee$ status and perspectives, arXiv:1108.2670.
[72] L. Calibbi, I. Galon, A. Masiero, P. Paradisi, and Y. Shadmi, Charged Slepton flavor post the 8 TeV LHC: A simplified model analysis of low-energy constraints and LHC SUSY searches, J. High Energy Phys. 10 (2015) 043..
[73] T. Sjostrand, S. Mrenna, and P. Z. Skands, A brief introduction to PYTHIA 8.1, Comput. Phys. Commun. **178**, 852 (2008).
[74] M. Cacciari, G. P. Salam, and G. Soyez, FastJet user manual, Eur. Phys. J. C **72**, 1896 (2012).
[75] M. Cacciari, G. P. Salam, and G. Soyez, The anti-k_t jet clustering algorithm, J. High Energy Phys. 04 (2008) 063.
[76] A. Djouadi, J.-L. Kneur, and G. Moultaka, SuSpect: A Fortran code for the supersymmetric and Higgs particle spectrum in the MSSM, Comput. Phys. Commun. **176**, 426 (2007).
[77] A. Djouadi, M. Muhlleitner, and M. Spira, Decays of supersymmetric particles: The Program SUSY-HIT (SUspect-SdecaY-Hdecay-InTerface), Acta Phys. Polon. **B38**, 635 (2007).
[78] S. Chatrchyan *et al.*, Identification of b-quark jets with the CMS experiment, J. Instrum. **8**, P04013 (2013).
[79] B. Gjelsten, D. Miller, and P. Osland, Measurement of SUSY masses via cascade decays for SPS 1a, J. High Energy Phys. 12 (2004) 003.
[80] N. Kidonakis, Top quark theoretical cross sections and pT and rapidity distributions, arXiv:1109.3231.
[81] J. M. Campbell, R. K. Ellis, and C. Williams, Vector boson pair production at the LHC, J. High Energy Phys. 07 (2011) 018.
[82] W. Beenakker, M. Klasen, M. Krämer, T. Plehn, M. Spira, and P. M. Zerwas, The Production of Charginos/Neutralinos and Sleptons at Hadron Colliders, Phys. Rev. Lett. **83**, 3780 (1999).